Use of Bauxite Residue Slurry as Single Activator in a Hybrid Binder System

Lukas Arnout[1], Tobias Hertel[1], Maxime Liard[2], Didier Lootens[3], and Yiannis Pontikes[4]
1. PhD candidate
4. Professor
KU Leuven, Department of Materials Engineering, Leuven, Belgium
2. Researcher
3. Principal Scientist
Sika Technology AG – Central Research, Zürich, Switzerland
Corresponding author: Lukas.Arnout@kuleuven.be

Abstract

The use of bauxite residue (BR) slurry as an activator in a hybrid system is explored in this paper. The strong alkaline nature of the slurry, which is considered as a major barrier for most valorization routes, is beneficial in this approach, where it is used as single source of water and alkalis to activate a hybrid cementitious precursor blend. Moreover, the fineness of the solid fraction of the slurry is expected to improve the particle packing, enabling the reduction of the water content and thus of the final system porosity. Experimentally, ≥ 33 wt% of BR slurry, was homogenized and subsequently mixed with either non-ferrous metallurgy slag or ground granulated blast furnace slag, ≤ 10 wt% of ordinary Portland cement and minor additives. The raw materials were mixed and the resulting pastes were cured at ambient conditions. Satisfactory mechanical properties were reached, exceeding 35 MPa already after 3 d of curing at room temperature. The results are promising, also considering that the slag mix can be potentially replaced by a thermally processed BR, thus leading to a maximization of total BR content in the newly formed binder.

Keywords: alkali/OPC activation, bauxite residue, red mud, non-ferrous metallurgy slag, GGBFS, mortar, mix design.

1. Introduction

Bauxite residue (BR) is the alkaline residue which is generated in a high volume, exceeding 150 Mt/year, during the Bayer process for the production of alumina [1]. Negative public perception, costs and scarcity of disposal areas, are some of the main drivers for research on the reuse of BR as resource for novel materials. Next to the recovery of base metals and rare earth elements from BR [2], the production of construction materials seems to be a reasonable way to incorporate large volumes of BR [3]. Various literature is published on using BR in geopolymers or inorganic polymer, a binder which is generally formed by the alkali activation of an aluminosilicate precursor [4]. Most studies dealing with the use of BR in geopolymers, suggest a combination of BR with other reactive raw materials, such as fly ash [5] or metakaolin [6]. In most of these cases dried BR was used which mainly acted as a fine filler material merely contributing physically to the strength and microstructure. A significant decrease in properties is reported when large volumes of BR are used. In order to activate BR so that it participates in the reactions for the inorganic polymers, different treatments, such as a chemical and thermal transformation [7] has proven to be a suitable alternative. Another approach was pursued by Krivenko *et al* [8] who prepared various alkaline cements including high fractions of BR with ground granulated blast furnace slag (GGBFS) and cement in combination with Na_2CO_3, sodium silicate or $Na_2O{\cdot}SiO_2{\cdot}5H_2O$ as alkaline components. Promising compressive strengths of 60 MPa were reached for mortar samples incorporating 60 wt% BR, 30 wt% GGBFS, 10 wt% OPC, activated using sodium silicate solution according to a liquid to solid ratio of 0.4. Several pressed concrete samples were prepared and up to 90 wt% of BR was incorporated in a mix with 9.2 wt% of GGBFS, 1.2 wt% of alkaline reagents with an addition of 16 wt% of water over the total mix. A compressive strength of 4 MPa was achieved after 28 d, while higher GGBFS contents lead to higher strengths. In another approach, spent Bayer liquor (= after Al-hydroxides removal) consisting mainly of NaOH and dissolved

Na-aluminates is used as alkaline activator of fly ash [9]. Satisfying compressive strength of about 42 MPa was reached after 28 d. The liquid fraction of BR slurry (as it leaves the Bayer process), which still consists of a considerable amount of alkaline liquid, is believed to act as an activator for the precursor materials.

In this paper a novel hybrid binder system is studied incorporating waste streams from different industries in a synergistic way. A bauxite reside slurry in an "as-produced" state from the Bayer process is used as an alkaline activator for a GGBFS or a non-ferrous metallurgical slag. NaOH additions and their influence on the total alkalinity and reactivity of the systems are investigated. OPC was added to accelerate the hydration by a rapid formation of hydration products in an alkaline environment. These hydration products potentially act as nucleation sites for the reaction products formed with the dissolved slag species and thus cause a faster strength development [8]. Basanite also proved to be beneficial for the strength development [10] whereas the workability was improved by adding superplasticizer.

2. Material and methods

2.1. Raw materials

A synthetic iron-silicate slag (NFMS) was produced by melting iron ore, quartz sand, limestone and chamotte at a temperature of 1300 °C followed by water quenching in order to obtain a glass with a chemistry comparable to non-ferrous metallurgical slags, such as copper, lead, zinc and ferro-nickel slag [11-13]. A commercial ground granulated blast furnace slag (GGBFS) from Orcem and a CEM I 52.5N from Vicat were used in this study as additions. Bauxite residue (BR) slurry was supplied from RUSAL Aughinish (Ireland). The solid content of the slurry was 59 wt%.

The chemical composition of all raw materials was analyzed using X-ray fluorescence and X-ray diffraction using the Rietveld method for the quantification of the data. Physical properties, such as specific surface area, particle size distribution and density were determined using a Blaine apparatus, a laser diffraction particle size analyzer and a helium pycnometer. The pH and the chemical composition of the liquid fraction of BR, obtained after filtering using 0.45 µm filter paper, was determined using a pH meter and an ICP-OES, respectively.

2.2 Preparation of Pastes and Mortars

Pastes of different compositions were prepared per 500 g in a 3 L Hobart mixer, first mixed for 1 minute at speed 1 and then 4 minutes at speed 2. 1000 kg/m³ of homogenized BR slurry is used as a base material and mixed with 1400 kg/m³ of GGBFS or 2000 kg/m³ of NFMS in order to obtain a similar rheological behavior of the different mixtures. More NFMS had to be added due to the higher density and broader particle size distribution compared to the GGBFS. Considering the liquid fraction of the BR slurry, a liquid to slag ratio of 0.205 for the NFMS samples and 0.293 for the GGBFS samples was used. When cement is added, 200 kg/m³ of the slag is replaced by CEMI 52.5N. In case of extra alkali activation, 20 kg/m³ of NaOH pellets (> 99 % purity, Sigma Aldrich) were added to the powder mix. 20 to 48 kg/m³ of non-commercial superplasticizer is used to keep the rheological properties of the slurries constant. The amount of superplasticizer was adapted for each mix to obtain a comparable workability. 12 kg/m³ of bassanite ($CaSO_4 \cdot 0.5\ H_2O$) from Knauf was added in all mixes, as this has proven to be beneficial for the strength development in NaOH/OPC activated slags [10]. The compositions in kg/m³ of the eight mixes prepared in this study are given in Table 1.

Mechanical strengths, of the pastes, are obtained from the acoustic reflection described by Lootens [14]. Initial setting and final setting times, respectively, are the moments when the strengths are 0.1 MPa and 1 MPa. Semi adiabatic calorimetry is used to obtain the heat evolution during the hardening phase of 400 g of paste. Mortars were prepared by mixing 1 kg of paste with 1 kg of masonry quartz sand with a maximum grain size of 1 mm for 4 minutes in a Hobart mixer and casted in 4 x 4 x 16 cm^3 mortar prisms. The compressive strength at 28 d was measured using an Instron 5985 applying a crosshead speed of 2 mm/min.

Table 1. Composition of the pastes in kg/m³. The wt% are indicated in brackets.

Sample	BR slurry	GGBFS	NFMS	CEM I	NaOH	$CaSO_4 \cdot 0.5H_2O$	plasticizer
GGBFS-B	1000 (41)	1400 (58)				12 (0.5)	20 (0.8)
GGBFS-OPC	1000 (41)	1200 (49)		200 (8.2)		12 (0.5)	32 (1.3)
GGBFS-Na	1000 (40)	1400 (56)			20 (0.8)	12 (0.5)	48 (1.9)
GGBFS-OPC-Na	1000 (40)	1200 (49)		200 (8.1)	20 (0.8)	12 (0.5)	40 (1.6)
NFMS-B	1000 (33)		2000 (66)			12 (0.4)	20 (0.7)
NFMS-OPC	1000 (33)		1800 (59)	200 (6.6)		12 (0.4)	32 (1.1)
NFMS-Na	1000 (32)		2000 (65)		20 (0.6)	12 (0.4)	48 (1.6)
NFMS-OPC-Na	1000 (33)		1800 (59)	200 (6.5)	20 (0.7)	12 (0.4)	40 (1.3)

3. Results and discussion

3.1 Raw Materials

The most prominent differences between the slags used are the high iron oxide content of the NFMS and the high CaO content of the GGBFS. Both slags have in common a considerable amount of silica as shown in Table 2. The dry fraction of the used BR consists mainly of iron, alumina and silica oxides, also reflected in its mineralogy summarized in Table 3.

Table 2. Chemical composition of the base raw materials (XRF).

Raw material	FeO_x	SiO_2	CaO	Al_2O_3	MgO	$(K,Na)_2O$	TiO_2	SO_3	LOI
NFMS	43.3 [(1)]	35.2	11.7	4.9	2.7	0.5	0.5	-	-
GGBFS	0.6 [(1)]	33.1	38.2	13.7	8.2	0.8	1.1	2.0	-
CEMI 52.5 N	4.9 [(2)]	20.7	64.2	3.5	0.9	0.6	0.2	2.3	1.4
Dried BR	43.6 [(2)]	11.7	5.5	19.3	0.1	8.8 Na_2O 0.1 K_2O	9.1	0.6	9.5

[(1)] calculated as FeO, [(2)] calculated as Fe_2O_3

The synthetic NFMS is 97 wt% amorphous while the GGBFS is fully amorphous. The characteristic clinker phases are found in OPC, among some calcium sulfate and calcite. The amorphous fractions of the slags and the clinker phases of OPC turn these into reactive materials, while the crystalline phases of BR are non-reactive or very poorly reactive in hydraulic and alkaline systems.

Table 3. Quantitative XRD analysis of raw materials; '–' implies not detected.

	NFMS	GGBFS	CEM I 52.5 N	Dried BR
Amorphous	97	100	-	-
C_3S	-	-	63.0	-
C_2S	-	-	17.6	-
C_3A	-	-	1.5	-
C_4AF	-	-	13.7	-
$C\hat{S}$	-	-	1.6	-
$C\hat{S} \cdot 2H$	-	-	1.0	-
$C\hat{C}$	-	-	1.2	2
Magnetite	3	-	-	-
Hematite	-	-	-	32
(Al)Goethite	-	-	-	20
Cancrinite	-	-	-	18
Gibbsite	-	-	-	10
Katoite	-	-	-	4
Rutile	-	-	-	2
Diaspore	-	-	-	2
Bayerite	-	-	-	2
Quartz	-	-	-	1

Boehmite	-	-	-	1
Anatase	-	-	-	1

*C = CaO, S = SiO_2, A = Al_2O_3, F = Fe_2O_3, $\hat{S}$ = SO_4, $\hat{C}$ = CO_2

Results of the particle size distribution analysis revealed that dried BR is considerably finer than the other materials, as shown in Figure 1. NFMS however has a higher specific surface area than GGBFS and OPC as seen in Table 4. The higher density of NFMS and the broader particle size distribution in comparison with GGBFS explains the different volumes used for the mix design described in Table 1.

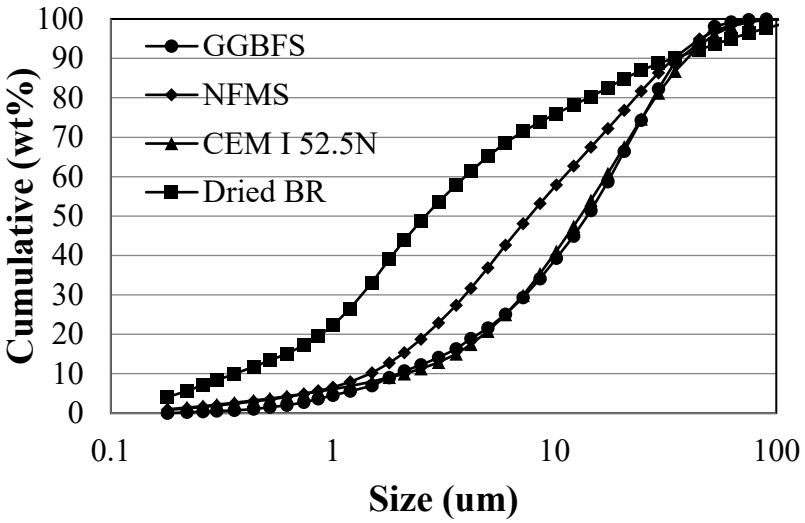

Figure 1. Cumulative particle size distributions of the raw materials.

Table 4. Physical characterization of the base raw materials.

Material	Density (g/cm³)	Blaine surface (cm²/g)	D_{10} (µm)	D_{50} (µm)	D_{90} (µm)
NFMS	3.55	5000 ± 250	1.5	8	35
GGBFS	2.91	4400 ± 220	1.8	12	30
CEM I 52.5N	3.11	4550 ± 230	2.1	13	40
Dried BR	2.76	-	0.4	2.7	35

A pH of 12.8 has been measured for the liquid fraction of the BR slurry. The ICP analysis shown in Table 5, demonstrates the presence of 2502 ppm Na^+ ions, corresponding to a 0.11 M NaOH solution. This molarity should theoretically lead to a pH of 13.0. The measured pH is lower than the theoretical value, due to the presence of dissolved alumina and carbonates which acidify the solution.

Table 5. ICP analysis of the BR liquor in ppm (mg/L).

Element	Na	Al	Si	Ca	Ti	Fe
ppm	2502	1052	4	3	0	<LOD

3.2 Paste and mortar characterization

Four different ways of activation are investigated and compared. A reference sample, named B, is made with slag and only BR slurry as activator. The samples with the suffix OPC and Na are activated with OPC or NaOH, respectively. Finally, a combined OPC-NaOH activation was carried out. The early strength development shows significant differences between the different activation routes as shown in

Figure 2 and 3, while some trends are visible when comparing both slags that are activated in the same way. The strength data are also summarized in Table 6.

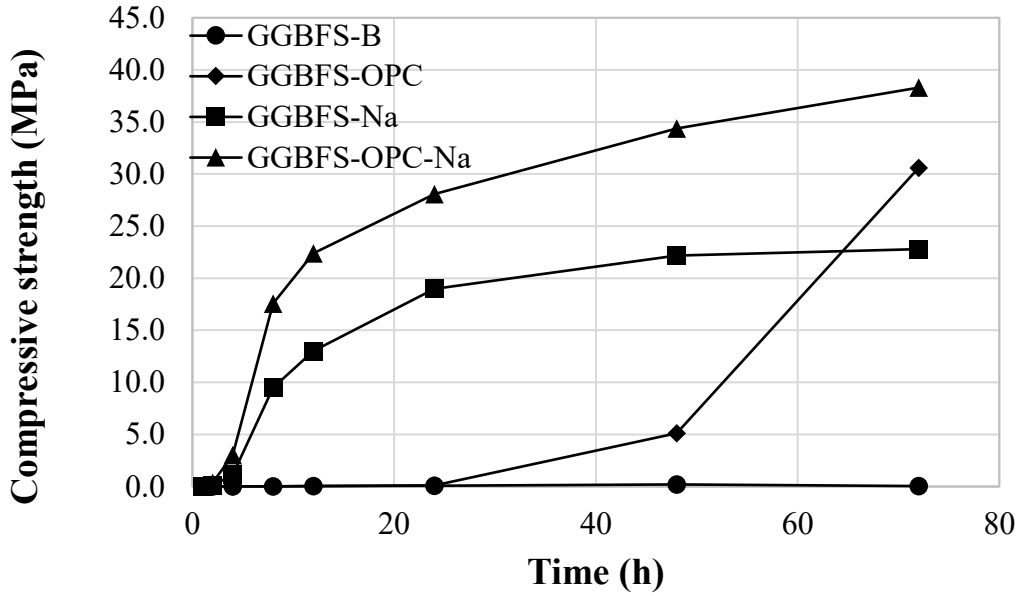

Figure 2. Early age compressive strength development of samples with GGBFS.

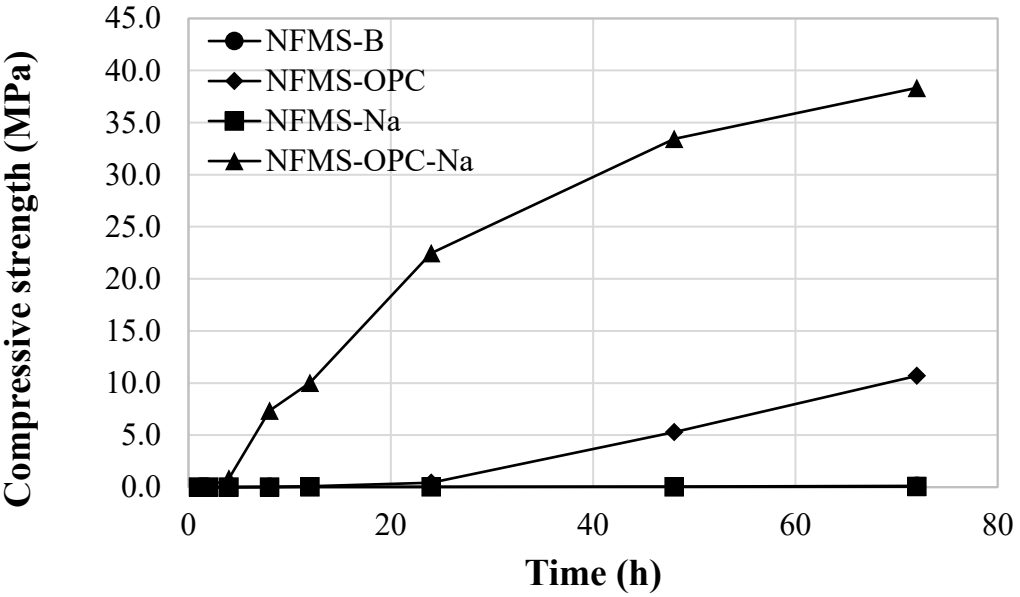

Figure 3. Early age compressive strength development of samples with NFMS.

Both reference samples GGBFS-B and NFMS-B have not reacted yet after 72 h. This means that the alkalinity of the BR liquor is not high enough to dissolve the slag effectively within that time. After 28 d of hardening the compressive strengths of the blank mortar samples is still very low, with 14 MPa for GGBFS-B and 6 MPa for NFMS-B as shown in Figure 4, demonstrating the limited reactivity of these systems. GGBFS shows a higher compressive strength than NFMS due to its higher basicity and faster dissolution in alkaline media.

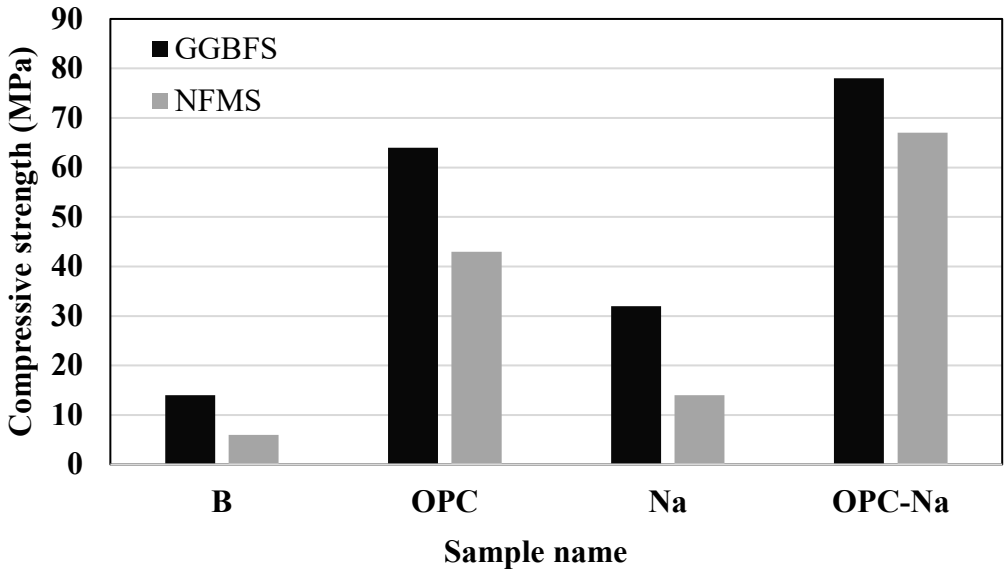

Figure 4. Compressive strength after 28 d of mortars prepared respecting a paste/sand ratio of 1.

Table 6. Compressive strength in MPa measured during the first 72 h of hardening.

	GGBFS-B	GGBFS-OPC	GGBFS-Na	GGBFS-OPC-Na	NFMS-B	NFMS-OPC	NFMS-Na	NFMS-OPC-Na
1 h	0.0	0.0	0.0	0.0	0.0	0.0	0.0	0.0
2 h	0.0	0.0	0.1	0.4	0.0	0.0	0.0	0.1
4 h	0.0	0.0	1.1	3.0	0.0	0.0	0.0	0.8
8 h	0.0	0.0	9.5	17.6	0.0	0.0	0.0	7.3
12 h	0.0	0.0	13.0	22.4	0.0	0.1	0.0	10.0
24 h	0.1	0.1	19.0	28.1	0.0	0.4	0.0	22.5
48 h	0.1	5.1	22.2	34.3	0.0	5.3	0.0	33.5
72 h	0.1	30.6	22.8	38.3	0.1	10.7	0.1	38.3

This hypothesis is supported by the observed strength development when additional NaOH is added to obtain a molarity of 1.36 M. In this case, GGBFS-Na already reaches 19 MPa after 24 h while NFMS-Na develops no strength after 72 h, confirming the large difference in dissolution kinetics between both slags. The compressive strength of GGBFS-Na seems to reach a plateau after 48 h with 23 MPa but an increase to 32 MPa for the mortar samples can be measured after 28 d (Figure 4). The initial and final setting time are 1.4 and 3.1 h, respectively, which is rather fast, compared to a normal OPC mortar (Table 7). Thus, it can be concluded that the reaction kinetics in sample GGBFS-Na are fast, but the formation of strength-giving products is rather low.

Table 7. Initial and final setting times of the different pastes in hours.

	GGBFS-B	GGBFS-OPC	GGBFS-Na	GGBFS-OPC-Na	NFMS-B	NFMS-OPC	NFMS-Na	NFMS-OPC-Na
I.S.	> 72	21	1.4	1.1	< 72	10.7	65	1.9
F.S.	> 72	36	3.1	2.2	< 72	24.6	> 72	3.4

The addition of OPC leads to increasing strength for both slags tested, compared to the systems without cement. Higher final strengths are reached while reaction kinetics are much slower with systems containing OPC. After 24 h, GGBFS-OPC and NFMS-OPC have not yet reached 1 MPa, while at 72 h they already reached respectively 30 and 11 MPa as shown in Figure 2 and 3. After 28 days the strength reached 64 and 43 MPa, which is satisfactory from an engineering point of view; however the late final

setting time of 31 h and 24.6 h, respectively, limits their use. To obtain the good final strength gained with the OPC activation together with the early strength development obtained during NaOH activation, two samples were prepared with a combined OPC/NaOH activation. Sample GGBFS-OPC-Na and NFMS-OPC-Na are self-leveling and have a respective final setting time of 2.2 and 3.4 h. An excellent 24 h compressive strength of respectively 28.1 and 22.5 MPa is combined with a 28 day mortar strength of respectively 78 and 67 MPa as shown in Table 6 and represented in the graphic of Figure 4.

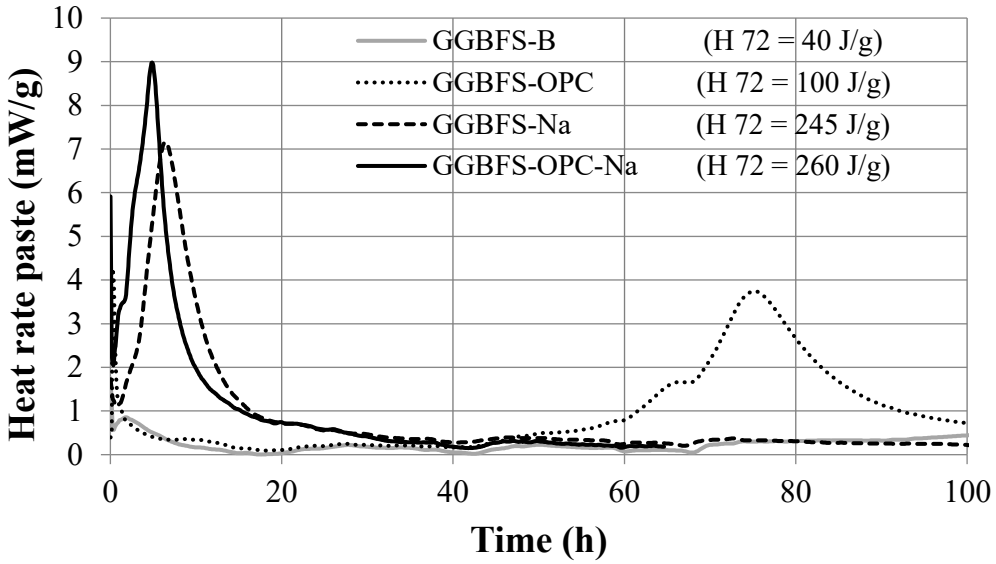

Figure 5. Early age adiabatic calorimetry results of samples with GGBFS in mW per gram of paste. The cumulative heat release after 72 h in J per gram paste (H 72) is given in between brackets.

No reaction peaks in the two series of calorimetric curves of Figure 5 and 6 are visible during the first 72 h for the reference samples, which is in line with the fact that both of them have not gained any strength during this period. The addition of 20 kg/m³ NaOH instead of 200 kg/m³ OPC leads to an accelerated reaction (Figure 5). The main reaction peak in sample GGBFS-Na appears after 5.7 h while the main reaction in sample GGBFS-OPC just takes place after 76 h. In GGBFS-OPC two peaks are detected: the first most likely corresponding to the hydration of OPC with a heat flow of 1.6 mW/g paste at 65 h and the second (3.75 mW/g paste) after 75 h, is associated with the dissolution and reaction of the slag. In GGBFS-Na, to the absence of OPC, only one distinct peak appears after 5.7 h due. As it can be seen in the graphic of Figure 6, no peaks are observed for NFMS-Na, which is in agreement with the fact that no strength is developed within the measured timeframe.

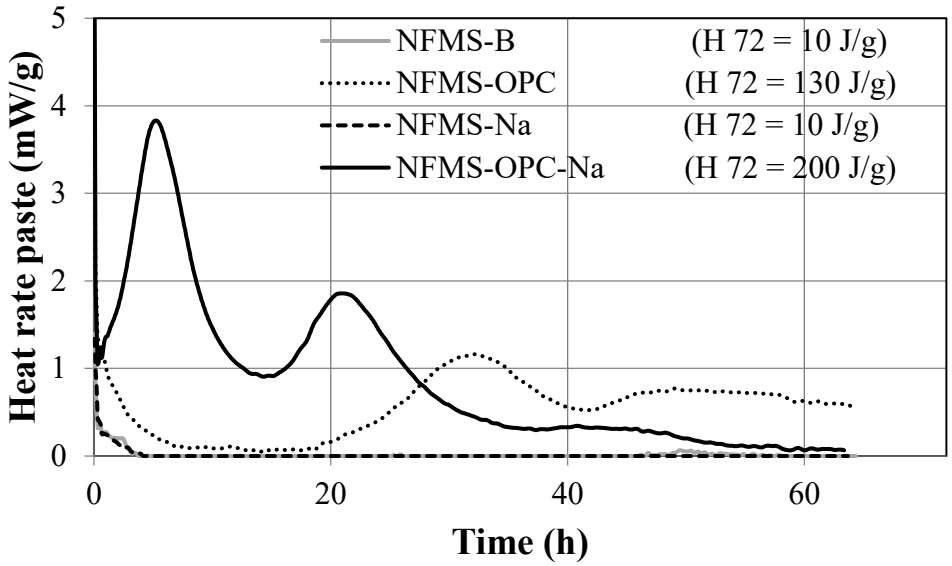

Figure 6. Early age adiabatic calorimetry results of samples with NFMS in mW per gram of paste. The cumulative heat release after 72 h in J per gram paste (H 72) is given in between brackets.

Although the strength development is slower for NFMS-OPC, the hydration peaks appear earlier compared to the GGBFS-OPC formulation. The acceleration can be caused by the fact that the 70 % more slag surface present, coming from the higher weight fraction in the mixes, can act as nucleation sites for the formation of hydration products of the OPC. The lower overall strength can be explained by the fact that the maxima of the heat peaks are four times smaller for the NFMS (1 mW/g) compared to the GGBFS (4 mW/g). The potential OPC hydration peak in the NFMS-OPC sample is higher than the slag reaction peak, which means that the OH^- concentration in the pore solution is not high enough to dissolve the low basicity NFMS. This low concentration of OH^- is caused by the limited solubility of $Ca(OH)_2$ in water. In opposition to the NFMS sample, the OPC hydration peak in the GGBFS-OPC sample is smaller than the slag hydration peak, meaning that the same OH^- concentration as in the NFMS samples is enough to dissolve the GGBFS, demonstrating the well-known latent hydraulic behavior of GGBFS. The same amount of hydration products in both samples is coming from the cement, but the NFMS is forming less strength-giving products ((C/N)-(F/A)-S-H gels) than the GGBFS, explaining the lower strength of the NFMS samples.

The calorimetry data of NFMS-OPC-Na revealed the OPC hydration and slag reaction peaks after 5 and 21 h, respectively. Most of the strength is gained during the slag reaction peak as shown in the Figure 3. Due the higher reactivity of GGBFS, the OPC and slag reaction peak in GGBFS-OPC-Na are nearly merged into one peak appearing after 5 h. Although the intensity of the peak (9 mW/g) is much higher than the NFMS-OPC-Na peaks (4 and 2 mW/g) the strength of both samples is similar. This is due to the fact that the NFMS-OPC-Na peaks are much broader, and thus show a longer but slower reaction than the GGBFS-OPC-Na peak resulting in a comparable cumulative heat release after 72 h of respectively 200 and 260 J/g of paste.

4. Conclusion

When combining NaOH activation with OPC, mortars from slags can be made with 500 kg/m³ of fresh BR slurry. Mortars with GGBFS deliver the highest strength at 28 d, but also with synthetic non-ferrous metallurgical slag a strength of 67 MPa was achieved with a self levelling mortar. NFMS slag can easily be replaced by thermally processed BR as proposed by Hertel et al. [7]. In this approach, mortars can be made with 500 kg/m³ of BR slurry combined with 1000 kg/m³ of ground granulated BR. When also the fine aggregates would be replaced by treated but unmilled BR, more than 1250 kg/m³ additional BR

can be incorporated. The best mortars in this study were activated with 100 kg/m³ OPC and 10 kg/m³ of NaOH, which is a low-cost and environmentally friendly way to valorize BR and non-ferrous metallurgical slags. Further research is focused on optimizing the activation, incorporating higher volumes of fresh slurry and evaluating the durability of such mortars.

Acknowledgements

The research leading to these results has received funding from the European Community's Horizon 2020 Programme (H2020/2014–2019) under Grant Agreement No. 636876 (MSCA-ETN REDMUD). This publication reflects only the authors' view, exempting the Community from any liability. Project website: http://www.etn.redmud.org.

5. References

1. K. Evans, The History, Challenges, and New Developments in the Management and Use of Bauxite Residue, *J. Sustain. Metall.,* Vol. 2, No. 4, (2016) 316–331.
2. C.R. Borra et al., Recovery of Rare Earths and Other Valuable Metals From Bauxite Residue (Red Mud): A Review. *J. Sustain. Metall.,* Vol. 2, No. 4, (2016) 365–386.
3. Y. Pontikes, G.N. Angelopoulos, Bauxite residue in cement and cementitious applications: Current status and a possible way forward, *Resources, Conservation and Recycling,* Vol. 73, (2013) 53–63.
4. P. Duxson et al., The role of inorganic polymer technology in the development of 'green concrete', *Cement and Concrete Research,* Vol. 37, No. 12, (2007) 1590–1597.
5. A. Kumar, S. Kumar, Development of paving blocks from synergistic use of red mud and fly ash using geopolymerization, *Construction and Building Materials,* Vol. 38 (2013) 865–871.
6. D.D. Dimas, I.P. Giannopoulou, D. Panias, Utilization of alumina red mud for synthesis of inorganic polymeric materials, *Mineral Processing and Extractive Metallurgy Review,* Vol. 30, No. 3, (2009) 211–239.
7. T. Hertel, B. Blanpain, Y. Pontikes, A Proposal for a 100 % Use of Bauxite Residue Towards Inorganic Polymer Mortar, *J. Sustain. Metall.,* Vol. 2, No. 4, (2016) 394–404.
8. P. Krivenko et al, Development of alkali activated cements and concrete mixture design with high volumes of red mud, *Construction and Building Materials,* Vol. 151, (2017) 819–826.
9. A. van Riessen et al., Bayer-geopolymers: An exploration of synergy between the alumina and geopolymer industries, *Cement and Concrete Composites,* Vol. 41, (2013) 29–33.
10. L. Arnout et al., NaOH-OPC activated lead slag, *in preparation*
11. B. Gorai, R.K. Jana, Premchand, Characteristics and utilization of copper slag – a review, *Resources, Conservation and Recycling*, Vol. 39, No. 4, (2003) 299-313.
12. V. Ettler, Primary phases and natural weathering of old lead-zinc pyrometallurgical slag from Pribam, Czech republic, *The Canadian Mineralogist,* Vol. 39 (2001) 873-888
13. K. Komnitsas, D. Zaharaki, V. Perdikatsis, Geopolymerisation of low calcium ferronickel slags, J. Mater. Sci., Vol. 42, (2007) 3073–3082
14. D. Lootens, Cimen ts et suspensions concentrées modèles. Écoulement, encombrement et floculation, PhD Université Pierre et Marie Curie-Paris VI, 2004.
15. Cement, U.S. Geological Survey, Mineral Commodity Summaries, January 2017
16. J. G. J. Olivier et al., Trends in global CO2 emissions: 2016 Report, PBL Netherlands Environmental Assessment Agency The Hague (2016), PBL publication number: 2315 European Commission, Joint Research Centre, Directorate Energy, Transport & Climate JRC Science for Policy Report: 103428